Current Research in Biotechnology 3 (2021) 135–146

Contents lists available at ScienceDirect

Current Research in Biotechnology

journal homepage: www.elsevier.com/locate/crbiot

Differences between common endothelial cell models (primary human aortic endothelial cells and EA.hy926 cells) revealed through transcriptomics, bioinformatics, and functional analysis

Dongdong Wang [a,*], Zhu Chen [b], Andy Wai Kan Yeung [c], Atanas G. Atanasov [d,e,f,*]

[a] Centre for Metabolism, Obesity and Diabetes Research, McMaster University, 1280 Main St. W., Hamilton, ON L8N 3Z5, Canada
[b] The Second Affiliated Hospital of Guizhou University of Traditional Chinese Medicine, Fei Shan Jie 32, 550003 Guiyang, China
[c] Oral and Maxillofacial Radiology, Applied Oral Sciences and Community Dental Care, Faculty of Dentistry, The University of Hong Kong, Hong Kong, China
[d] Department of Biotechnology and Nutrigenomics, Institute of Genetics and Animal Biotechnology of the Polish Academy of Sciences, 05-552 Jastrzębiec, Poland
[e] Ludwig Boltzmann Institute for Digital Health and Patient Safety, Medical University of Vienna, Spitalgasse 23, 1090 Vienna, Austria
[f] Department of Pharmacognosy, University of Vienna, Althanstrasse 14, 1090 Vienna, Austria

ARTICLE INFO

Keywords:
Endothelial cells
Bioinformatics analysis
Rap1 signaling pathway
Ras signaling pathway
HDL cellular association

ABSTRACT

Endothelial cells (ECs) are involved in various physiological process. Both primary human ECs and immortal endothelial cells are used in various studies. Available genomic or transcriptomic information for difference in ECs is deficient. Therefore, in this study we aim to reveal the difference between primary human aortic ECs (HAECs) and immortal EA.hy926 cells. We identified 529 differentially expressed genes (DEGs) between HAECs and EA.hy926 cells. Gene Ontology (GO), KEGG Pathway and GSEA enrichment analysis suggest that DEGs highly expressed in HAECs are distributed in Rap1 signaling pathway and Ras signaling pathway, which are contributing to the endothelial barrier function and endocytosis, among other functions. We also established long non-coding (lncRNA)-miRNA-mRNA ceRNA network, and further set up protein–protein interaction (PPI) network. High-density lipoprotein (HDL) cellular association experiments were verified that HAECs have stronger response to HDL cellular binding and endocytosis compared to EA.hy926 cells. This study identified DEGs between HAECs and EA.hy926 cells, and found enrichment of the Ras signaling pathway and Rap1 signaling pathway in HAECs, established ceRNA network and suggested that HAECs may have a stronger response to endothelial binding and endocytosis compared to EA.hy926 cells. This work provides a genomic basis to choose suitable EC model to reach respective research goals.

1. Introduction

Blood vessels transport oxygen and nutrients to other organs of the body, remove waste and carbon dioxide from different tissues, secrete angiocrine factors in different conditions, and serve as barrier for blood cells, cytokines and other factors (Potente et al., 2011). The inner layer of vessels is called tunica intima (endothelium), which is composed of a single layer of squamous endothelial cells (ECs) (Falkenberg et al., 2019). ECs are involved in the regulation of coagulation, vascular hemodynamics, vascular permeability, blood cell trafficking, and immunity, among others (Shao et al., 2020). Dysfunction of ECs has been reported to be associated with various diseases, such as cardiovascular diseases (CVDs) (Shao et al., 2020), cerebrovascular disease (Chrissobolis et al., 2011), cancer (Van Dreden et al., 2017), diabetes (Tabit et al., 2010), kidney disease (Malyszko, 2010), blinding eye disease (Campochiaro, 2013) and pulmonary arterial hypertension (Voelkel and Gomez-Arroyo, 2014).

To find potential targets in ECs to treat diseases, thousands of research works used human ECs as models (Uhrin et al., 2018; Wang et al., 2020; Wang et al., 2018). These human cell models are categorized in two types: 1) primary ECs including Human Aortic Endothelial cells (HAECs), Human Coronary Artery Endothelial Cells (HCAECs), Human Umbilical Vein Endothelial Cells (HUVECs), Human Umbilical Artery Endothelial Cells (HUAECs), Human Dermal Lymphatic Microvascular Endothelial Cells (HMVECs-dLyAd), Human Cardiac Microvascular Endothelial Cells (HMVEC-C), Human Pulmonary Artery Endothelial Cells (HPAEC) and among others, as well as 2) immortal endothelial cell lines, such as EA.hy926 and HMEC-1 cell

* Corresponding authors at: Department of Biotechnology and Nutrigenomics, Institute of Genetics and Animal Biotechnology of the Polish Academy of Sciences, 05-552 Jastrzębiec, Poland (A.G. Atanasov).
E-mail addresses: wangd123@mcmaster.ca (D. Wang), atanas.atanasov@univie.ac.at (A.G. Atanasov).

https://doi.org/10.1016/j.crbiot.2021.05.001
Received 21 December 2020; Revised 29 March 2021; Accepted 1 May 2021

2590-2628/© 2021 The Author(s). Published by Elsevier B.V.
This is an open access article under the CC BY license (http://creativecommons.org/licenses/by/4.0/).

lines (Ahn et al., 1995). Compared to primary human ECs which have a limited lifespan and display characteristics that differ from batch to batch, immortal endothelial cell lines are easier to be maintained and cultured, as well as more stable (Bouis et al., 2001). EA.hy926 cells have been widely used in various studies on ECs (Kaissarian et al., 2018; Kraehling et al., 2016; Yu et al., 2019). Although EA.hy926 cells preserve similar characteristics with primary human endothelial cells, such as HAECs (Ahn et al., 1995; Thornhill et al., 1993), it is worth to notify that there are different expression patterns in different ECs (Chi et al., 2003). Nevertheless, available genomic or transcriptomic information for difference in EC models is deficient. Therefore, in this study we aim to reveal the difference between HAECs and EA.hy926 cells by genome-wide expression assay.

Genome-wide expression profiling is being increasingly applied to dissect the complex difference among cells/tissues. RNA-seq is a powerful high-throughput DNA sequencing platform, which provides an unbiased and high sequencing depth analysis of the genome and transcriptome (Mortazavi et al., 2008). Application of RNA-seq has revealed the complexity of the transcriptomes of eukaryotic cells/tissue (Gustincich et al., 2006; Pan et al., 2008), and indicated that many transcripts have escaped our observation before (Ji et al., 2020). In the present study, we used RNA-seq technology and performed bioinformatic analysis to identify differentially expressed genes (DEGs) and differently regulated pathways between HAECs and EA.hy926 cells, established long non-coding (lncRNA)-miRNA-mRNA ceRNA network and further verified our findings by high-density lipoprotein (HDL)-endocytosis experiments. This study may provide a genomic basis for investigators to choose suitable EC models to reach their research goals.

2. Materials and methods

2.1. Cell culture

Human aortic endothelial cells (HAECs, ThermoFisher, Cat no.: C-006-5C) were cultured in Medium 200 (ThermoFisher, Cat no.: M200500) with low serum growth supplement kit (ThermoFisher, Cat no.: S003K), benzylpenicillin 100 U/mL and streptomycin 100 μg/mL at 37 °C in a humidified 5% CO_2, 95% air incubator. HAECs at passage number 5 were used for experiments.

EA.hy926 endothelial cells (ATCC® CRL2922™) were cultured in DMEM medium (with 4.5 g/L glucose), supplemented with 10% heat-inactivated FBS, benzylpenicillin 100 U/mL, streptomycin 100 μg/mL, and L-glutamine 2 mM at 37 °C in a 5% CO_2 incubator. EA.hy926 cells at passage number 5 were used for experiments.

2.2. RNA extraction and sequencing

HAECs and EA.hy926 cells were seeded at a density of 0.8×10^6 cells/well in 6-well plates for 72 h. The cells were then lysed in TRI reagent™ solution (Invitrogen, Cat no.: AM9738) according to the manufacturer's instruction. Total RNA was extracted by using RNAqueous™ Total RNA Isolation Kit (Invitrogen, Cat no.: AM1912). Concentrations of total RNA were measured with NanoDrop 2000 (ThermoFisher). There are three independent biological replicates in each condition. RNA quality was examined on an Agilent 2100 Bioanalyzer (Agilent) using the RNA 6000 Nano Kit. RNA integrity numbers (RINs) of the samples ranged between 8.9 and 9.5. cDNA was prepared from isolated RNA by using the NEBNext® Ultra™ II Directional RNA Library kit, and was subjected to next-generation sequencing from both ends with the Illumina HiSeq-1500 platform. Clean data were mapped by Hisat2. The raw counts were quantified to obtain the fragments per kilobase of transcript per million (FPKM) by the sequencing company Bluecape Scientifci (Beijing, China).

2.3. Data preprocessing and DEG analysis

The data were processed and analyzed with the statistical language R. We transferred FPKM to TPM (transcripts per kilobase million). The genes with TPM values < 1 in three biological replicates in both cell types were regarded as low expression and removed from the dataset. Principal component analysis (PCA) and cluster analysis were performed to verify the data quality. To check whether it is valuable to further perform DEG analysis, we compared the 2000 highly expressed genes between HAECs and EA.hy926 cells and showed total difference of genes between the two groups by heatmap.

DEG analysis was performed by using the limma/voom package (Law et al., 2014). DEGs were identified using the following threshold: $|\text{fold change}| > 2 \sim 3 \times$ standard deviation of $\log_2$(fold change), p-value < 0.01 and adjusted p-value < 0.05.

2.4. Gene Ontology (GO), KEGG pathway and GSEA enrichment

Over representation analyses (GO enrichment analysis and Kyoto Encyclopedia of Genes and Genomes (KEGG) analysis) were used to perform functional enrichment analysis. GO enrichment analysis of the DEGs was implemented by GOstats packages (https://bioconductor.org). GO annotation results were bar-plotted using the R software. The results were illustrated in a gene-concept network diagram by using cnetplot package (https://bioconductor.org).

The assignment of KEGG pathways to the transcripts was done through KEGG.db packages (https://bioconductor.org) to uncover the most significantly enriched pathways based on the DEGs. KEGG results were dot-plotted using the R software. The Pathview package was used to construct the network of enriched pathways.

We further performed functional enrichment analysis by Gene Set Enrichment Analysis (GSEA), which aggregates the per gene statistics across genes within a gene set to possibly detect situations where all genes in a predefined set change in a small but coordinated way (Subramanian et al., 2005). GSEA was performed by using gseKEGG function in R software, and the results were visualized by Ridgeplot and Enrichplot packages.

2.5. Establishment of the ceRNA network

The long non-coding (lncRNA)-miRNA-mRNA ceRNA network was constructed based on the hypothesis that lncRNAs directly interact with and regulate the activity of mRNAs by acting as miRNA sponges (Ala et al., 2013). Based on this hypothesis, we established the lncRNA-miRNA-mRNA ceRNA network in three steps.

2.5.1. Differential expression analysis of lncRNA, miRNA and mRNA

Differential expression analysis of lncRNA, miRNA and mRNA was performed by using the limma/voom package (Law et al., 2014) with the following threshold: $|\text{fold change}| > 1$ and p value < 0.05 for both lncRNA and miRNA analyses, as well as $|\text{fold change}| > 3$ and p value < 0.01 for mRNA analysis to obtain differently expressed lncRNAs (DElncRNAs), differently expressed miRNAs (DEmiRNAs), and differently expressed mRNAs (DEmRNAs), respectively.

2.5.2. Screening of potential miRNAs targeted by DElncRNAs

The predicted miRNAs targeted by the DElncRNAs were predicted by the miRcode online tool (http://www.mircode.org). The potential miRNAs targeted by the DElncRNAs were produced by matching the predicted miRNAs with DEmiRNAs from the experiments.

2.5.3. Screening of potential mRNAs targeted by the potential miRNAs

The predicted mRNAs targeted by potential miRNAs were predicted by the MiRDB (http://www.mirdb.org/) and Targetscan (http://www.targe tscan.org/) programs. The potential mRNAs

targeted by the potential miRNAs were produced by matching the predicted mRNAs with DEmRNAs from the experiments.

Finally, the potential miRNA and mRNAs were regulated by the DElncRNAs were selected to build the ceRNA network and lncRNA-miRNA-mRNA ceRNA network is visualized by Cytoscape (version 3.8.0).

2.5.4. Establishment of protein–protein interaction (PPI) network

For better understanding the relationship among targeted mRNAs in the ceRNA network, the PPI network was established by using the STRING database (Szklarczyk et al., 2017). The combined score of 0.4 was regarded as the cut-off criterion and the PPI was visualized.

2.6. Cellular association of HDL with ECs

To confirm the difference in endocytosis between HAECs and EA.hy926 cells, the HDL cellular association assay was performed as previously described (Wang et al., 2020). The radiolabeled ^{125}I-HDL was kindly prepared and provided by Prof. Wang (Sichuan University, China). HAECs and EA.hy926 cells were seeded at a density of 0.1×10^6 cells/well in 24-well plates for 48 h. Cells were then treated with cytochalasin D (Sigma, C8273) or control (0.1% DMSO) for 24 h. Then, cells were incubated with 10 μg/mL of ^{125}I-HDL in serum-free DMEM medium with 0.1% BSA for 1 h at 37 °C to obtain total HDL cellular association. To obtain unspecific HDL cellular association, the cells were incubated with both 10 μg/mL of ^{125}I-HDL and 400 μg/mL (40 ×) of non-labeled HDL in DMEM medium. Specific HDL cel-

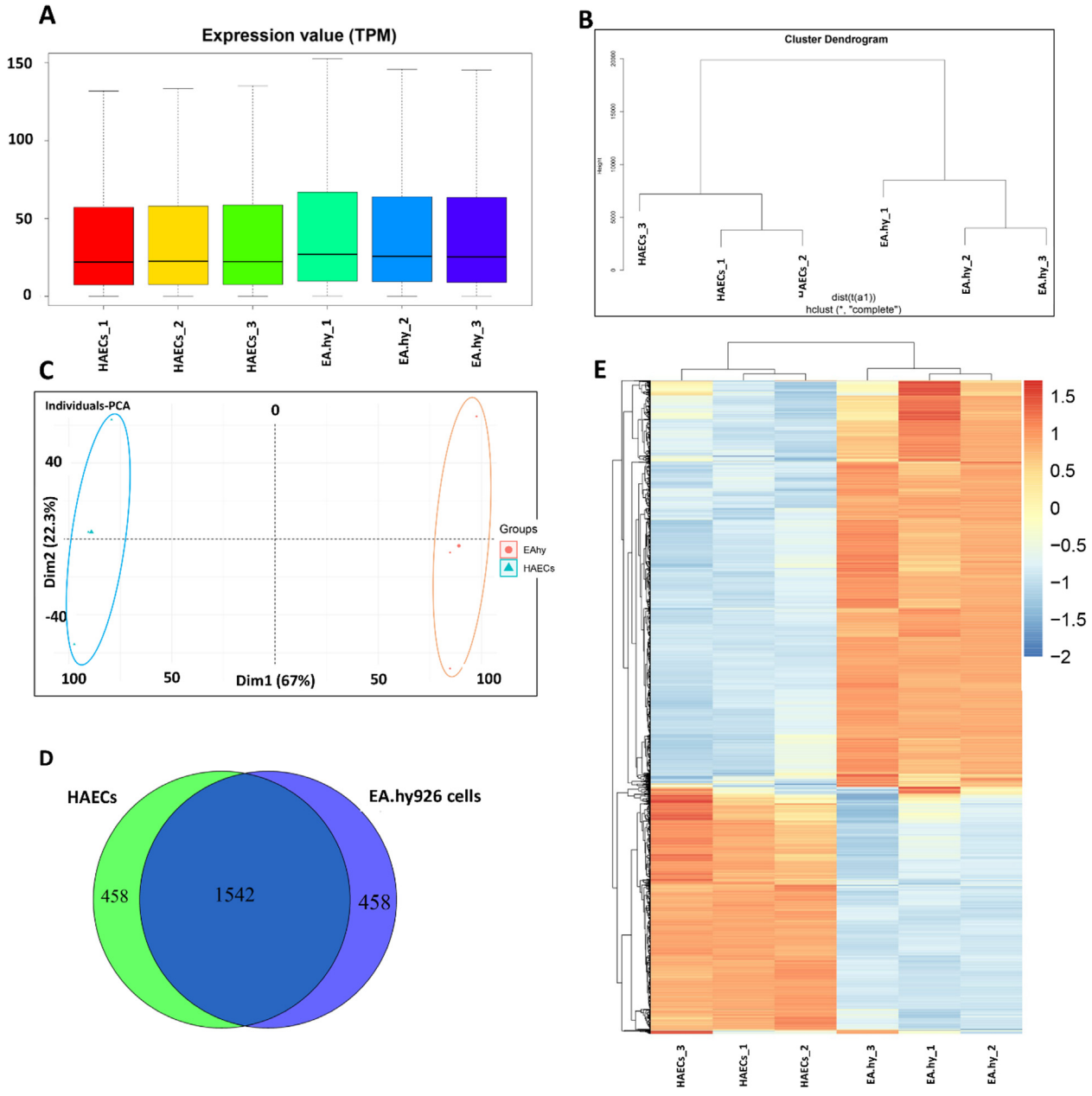

Fig. 1. RNA-seq data quality. (A) The average TPM of all gene expression in three biological replicates in both HAECs and EA.hy926 cells does not display significant difference. (B) The cluster analysis indicated that HAECs and EA.hy926 cells are categorized in the different groups, respectively. (C) PCA analysis shows that the different cell types HAECs and EA.hy926 cells are distinctly separated. (D) The Venn diagram displays 458 different genes (22.9%) in 2000 highly expressed genes set between HAECs and EA.hy926 cells. (E) The heatmap shows the total difference of gene expression between HAECs and EA.hy926.

lular association = (The total value - unspecific value)/protein content. Protein concentrations were tested by BCA assay.

3. Results

3.1. RNA-seq data quality

We transferred FPKM to TPM, and removed the genes with TPM values < 1 in three biological replicates in both HAECs and EA.hy926 cells. The average TPM of all gene expression in three biological replicates in both cell types did not have significant difference (Fig. 1A), which indicated that the data are possible to do further comparison. The results of cluster analysis and PCA showed that same cell types are clustered in the same group, and the different cell types are distinctly separated (Fig. 1B and C). As shown in Fig. 1D, there are 458 different genes (22.9%) in 2000 highly expressed genes set between HAECs and EA.hy926 cells, suggesting that it is valuable to further perform DEG analysis. We also showed total difference of gene expression between the two groups by heatmap (Fig. 1E).

3.2. Differential gene expression profile

After DEG analysis, a total of 529 genes were found to be differentially expressed between HAECs and EA.hy926 cells with threshold: $|\log_2(\text{fold change})| > 2.322$ (2 fold of SD), p-value < 0.01 and adjusted p-value < 0.05. Among them, 327 different genes were highly expressed in HAECs, while 202 different genes were highly expressed in EA.hy926 cells (Supplementary files 1 and 2). Volcano plots of the comparison between the two cell types showed the distributions of the intensities (Fig. 2A). The top 100 DEGs were showed in the Fig. 2B.

3.3. GO enrichment analysis

To further reveal the molecular characterization of the DEGs, GO annotation was used to analyze the DEGs with pvalueCutoff = 0.05, qvalueCutoff = 0.05. The GO database contains three main branches: biological process (GO_BP), molecular function (GO_MF), and cellular component (GO_CC). All the GO terms lists obtained in each category are summarized in Fig. 3. The detailed data are shown in the Supplementary files 3 and 4.

Specifically, DEGs highly expressed in HAECs are involved in 47 terms of GO_BP (Fig. 3A). These biological processes in HAECs mainly included cell adhesion, extracellular matrix (ECM) structure/organization, endothelial cell proliferation/development/migration, vascular development, Ras protein signal transduction, coagulation/hemostasis, renal system development and so on. Whereas, DEGs highly expressed in EA.hy926 cells are involved in 3 terms of CO_BP (Fig. 3B), including transmembrane receptor protein tyrosine kinase (RTK) activity, and reproductive development.

Regarding GO_MF, we found terms from the DEGs highly expressed in HAECs mainly implicated in ECM constituent, growth factor/collagen/cytokine binding, which are consistent with the results of GO_BP. In addition, the DEGs highly expressed in EA.hy926 cells were involved only in integrin binding which may be related to RTK activity (Klemke et al., 1994).

In GO_CC, the DEGs highly expressed in EA.hy926 cells are involved in 2 terms, namely collagen-containing ECM and basement membrane, which are also present in GO_CC terms related to DEGs highly expressed in HAECs. Besides, GO_CC terms enriched in DEGs highly expressed in HAECs included focal adhesion, cell–cell/substrate junction, various lumens (e.g., endoplasmic reticulum lumen, vesicle lumen, secretory granule lumen).

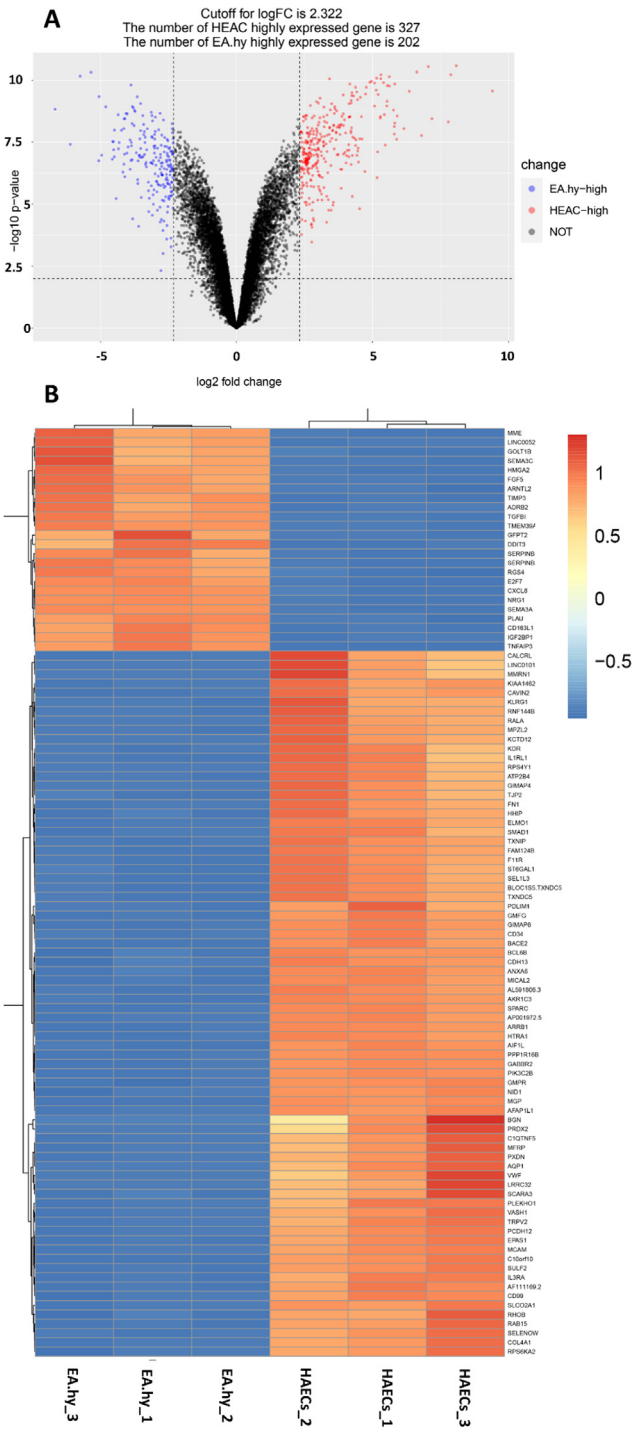

Fig. 2. Differential gene expression profile between HAECs and EA.hy926 cells. (A) The Volcano plot comparing the levels of gene expression between the HAECs and EA.hy926 cells. (B) The heatmap shows the top 100 DEGs between the HAECs and EA.hy926 cells.

To further understand the GO annotation, we analyzed the all DEGs between HAECs and EA.hy926 cells with pvalueCutoff = 0.01, qvalueCutoff = 0.05 and illustrated in a gene-concept network diagram (Fig. 3C). Consistent with the data above, 5 main GO terms are enriched based on all DEGs, including cell–cell adhesion via plasma-

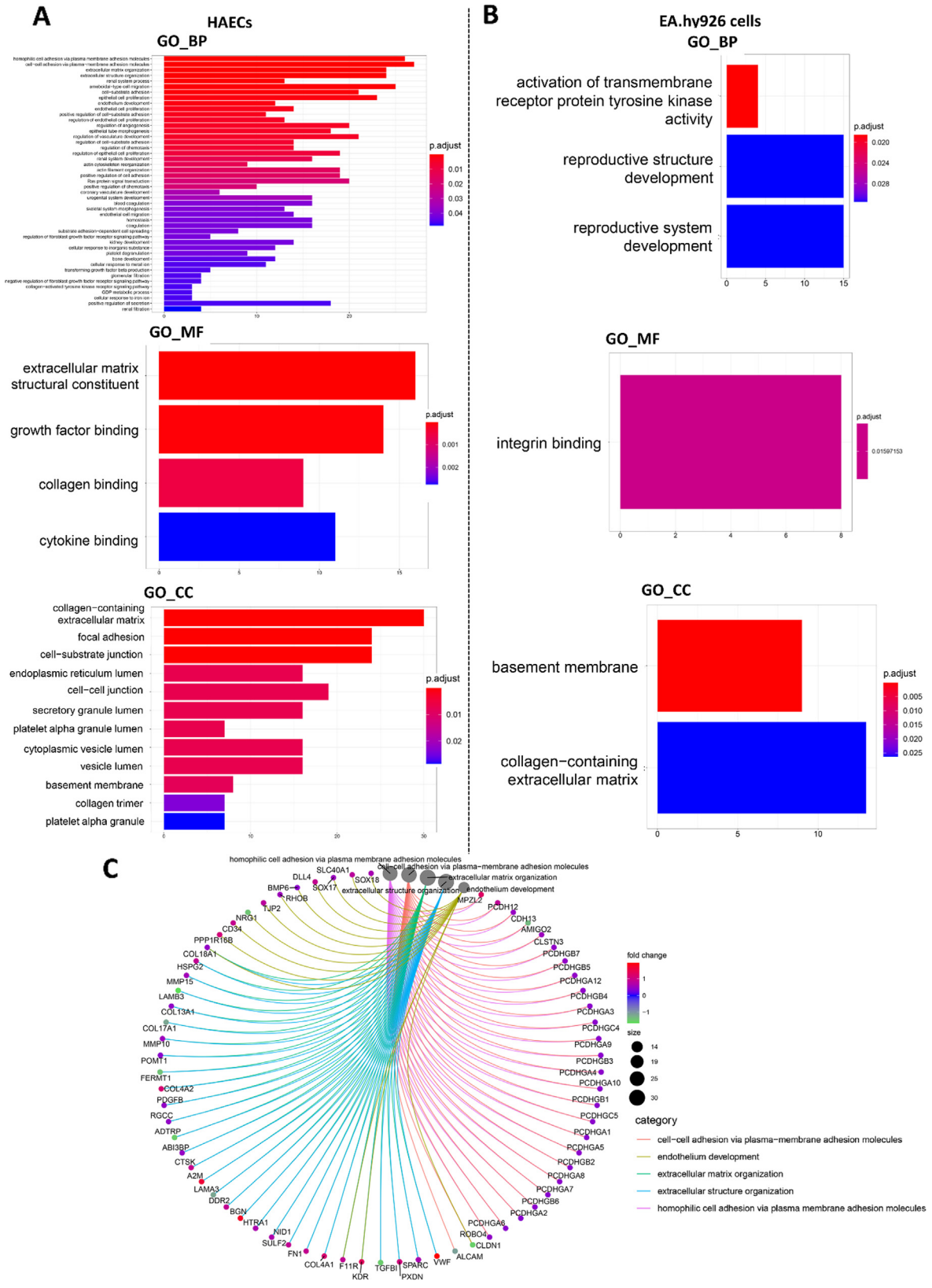

Fig. 3. The results of GO enrichment analysis. (A) DEGs highly expressed in HAECs are involved in 47, 4, and 12 terms of biological process (BP), molecular function (MF), and cellular component (CC) in GO, respectively. (B) DEGs highly expressed in EA.hy926 are involved in 3, 1, and 2 terms of biological process (BP), molecular function (MF), and cellular component (CC) in GO, respectively. (C) The gene-concept network diagram indicates DEGs between HAECs and EA. hy926 cells and the corresponding enriched GO terms.

Fig. 4. The results of KEGG pathway enrichment analysis. (A) The DEGs between HAECs and EA.hy926 cells are significantly enriched in 58 pathways. (B) The DEGs highly expressed in HAECs are distributed in 4 pathways. (C) The DEGs highly expressed in EA.hy926 cells are distributed in 7 pathways. (D) MAPK signaling pathway (KEGG ID hsa04010). (E) Rap1 signaling pathway (KEGG ID hsa04015). (F) Ras signaling pathway (KEGG ID hsa04014).

membrane adhesion molecules, ECM organization, extracellular structure organization, homophilic cell adhesion via plasma membrane adhesion molecules, and endothelium development.

3.4. KEGG pathway enrichment analysis

To further understand the signal pathways where the DEGs are distributed, a KEGG pathway enrichment analysis was performed. Firstly, a total of DEGs between HAECs and EA.hy926 cells were mapped to KEGG pathways, of which 58 pathways were significantly enriched (Fig. 4A and Supplementary file 5). There were several top significantly enriched pathways, including MAPK signaling pathway, Rap1 signaling pathway, Ras signaling pathway, focal adhesion, among others (Fig. 4A). Furthermore, the DEGs highly expressed in HAECs are distributed in 4 pathways, including Rap1 signaling pathway, Ras signaling pathway, and platelet activation (Fig. 4B). The DEGs highly expressed in EA.hy926 cells are distributed in 7 pathways, including MAPK signaling pathway, Cell cycle, Homologous recombination and DNA replication (Fig. 4C).

To further know the functions of top significantly enriched pathways in endothelial cells, we used the Pathview package to construct the network of the enriched pathways, namely KEGG ID hsa04010

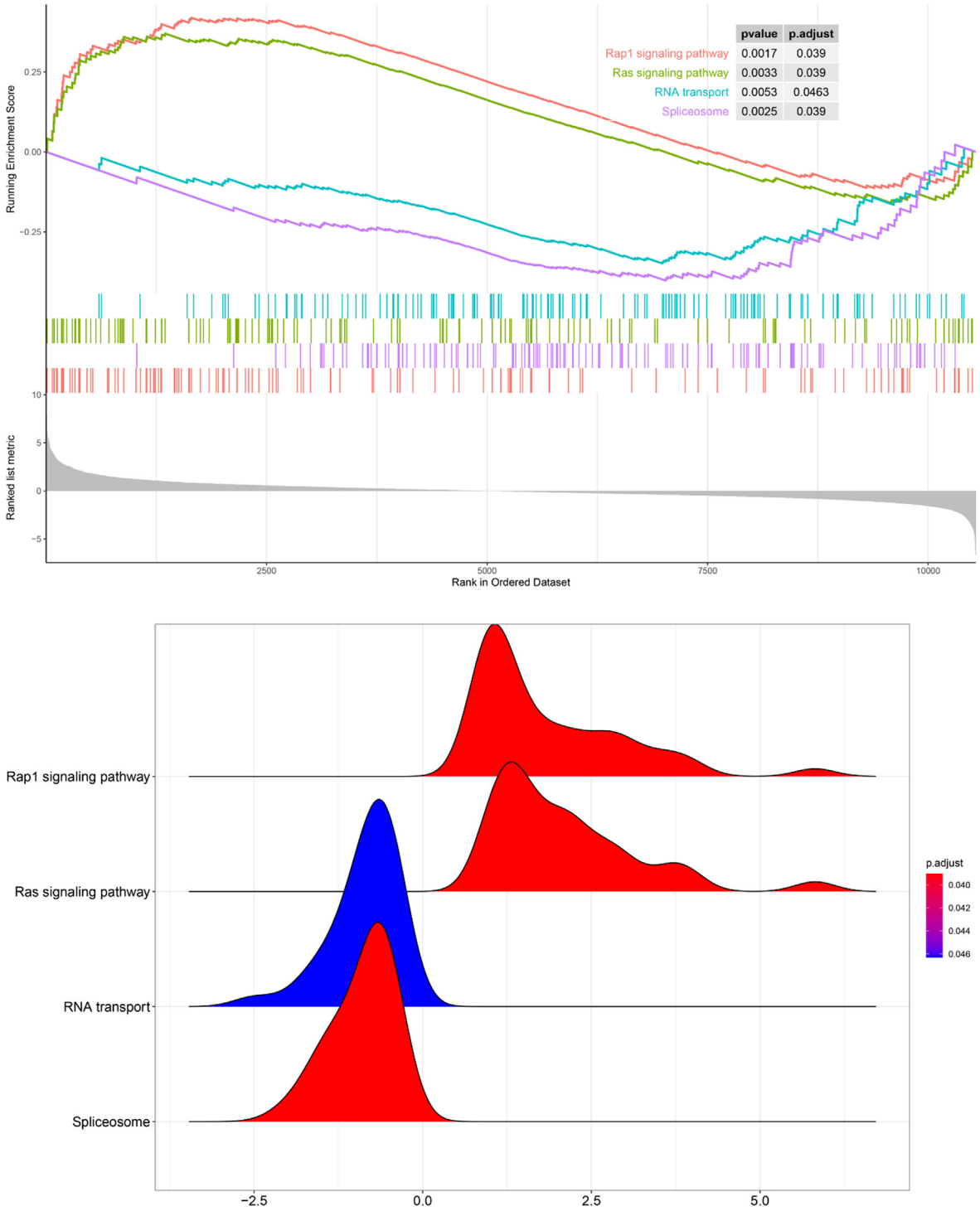

Fig. 5. The results of GSEA enrichment analysis. The two pathways (Ras signaling pathway and Rap1 signaling pathway) are enriched in HAECs. Another two pathways (RNA transport and Spliceosome) are enriched in EA.hy926 cells.

(MAPK signaling pathway) (Fig. 4D), KEGG ID hsa04015 (Rap1 signaling pathway) (Fig. 4E), and KEGG ID hsa04014 (Ras signaling pathway) (Fig. 4F). These data suggest that MAPK signaling pathway enriched in EA.hy926 cells contributed to the cell cycle and proliferation. While Ras signaling pathway enriched in HAECs contributed to endocytosis, cell–cell junction, cell migration and so on, and Rap1 signaling pathway enriched in HAECs contributed to cell adhesion, migration, and proliferation, among others.

3.5. GSEA enrichment analysis

We further performed functional enrichment analysis of all genes by GSEA. As shown in Fig. 5, we found that two pathways (Ras signaling pathway and Rap1 signaling pathway) are enriched in HAECs, which is consistent with results from KEGG pathway enrichment analysis. Another two pathways (RNA transport and Spliceosome) are enriched in EA.hy926 cells, based on all gene changes.

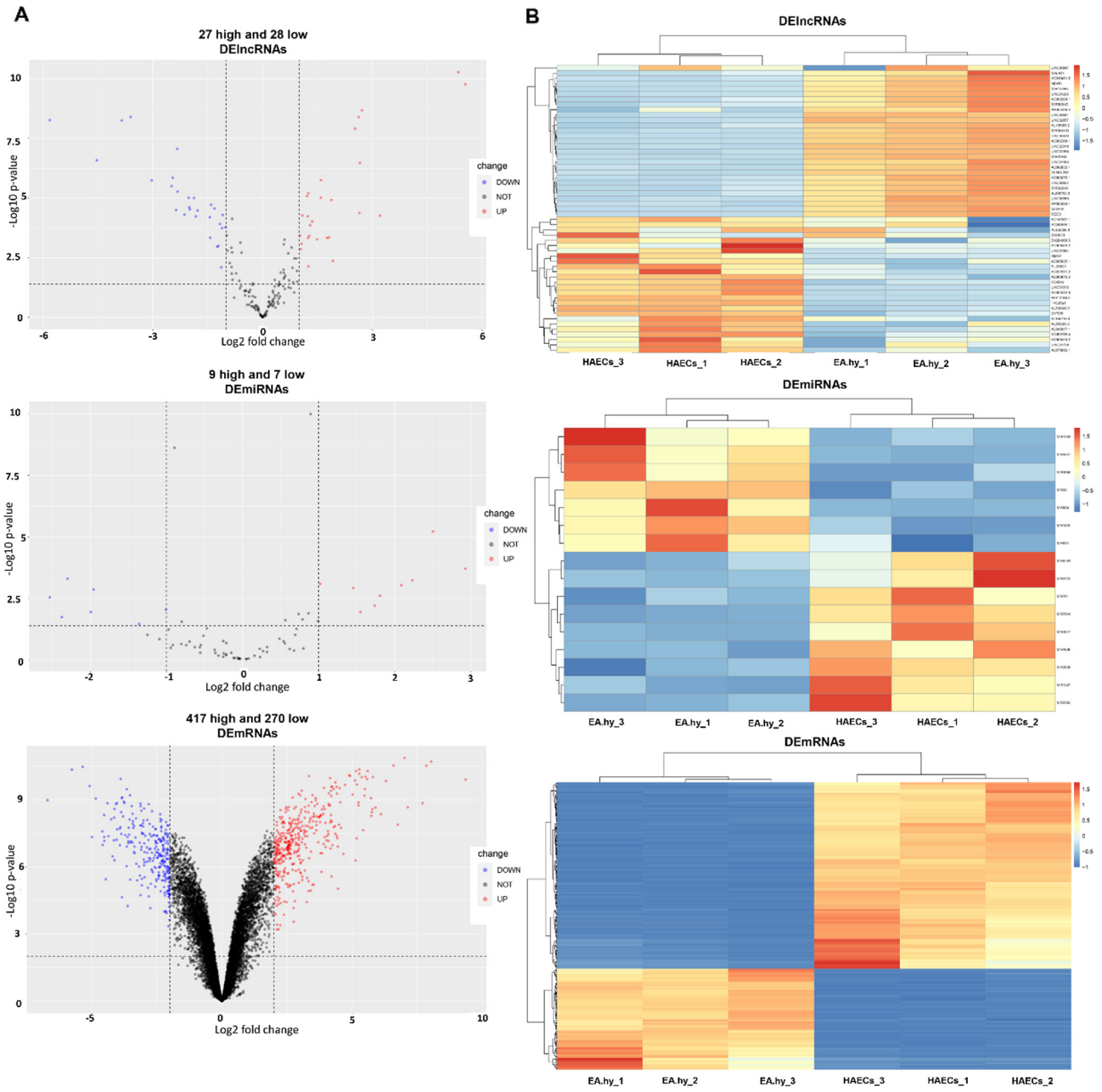

Fig. 6. Identification of DElncRNAs, DEmiRNAs, and DEmRNAs by DEG analysis. (A) Volcano plots display the distribution of the DElncRNAs, DEmiRNAs, and DEmRNAs. A total of 55 DElncRNAs (27 highly and 28 lowly expressed genes), 16 DEmiRNAs (9 highly and 7 lowly expressed genes), and 687 DEmRNAs (417 highly and 270 lowly expressed genes) were identified in HAECs compared to EA.hy926 cells. (B) The heat maps show clear separation and consistency in the expression profiles of DElncRNAs, DEmiRNAs, and DEmRNAs between the HAECs and EA.hy926 cells.

3.6. Establishment of the ceRNA network and PPI network

We firstly identified DElncRNAs, DEmiRNAs, and DEmRNAs by DEG analysis. A total of 55 DElncRNAs (27 highly and 28 lowly expressed genes), 16 DEmiRNAs (9 highly and 7 lowly expressed genes), and 687 DEmRNAs (417 highly and 270 lowly expressed genes) were identified in HAECs, compared to EA.hy926 cells. Volcano plots displaying the distribution of the DElncRNAs, DEmiRNAs, and DEmRNAs were generated, as shown in Fig. 6A. The heat maps showed clear separation and consistency in the expression profiles of DElncRNAs, DEmiRNAs, and DEmRNAs between the HAECs and EA.hy926 cells (Fig. 6B and Supplementary file 6).

As shown in Supplementary file 7A, we found around 100 predicted miRNAs targeted by the DElncRNAs by using the miRcode online tool. When matching the predicted miRNAs with DEmiRNAs from the experiments, only 2 potential miRNAs (hsa-miR-22-3p and hsa-miR-130b-3p) were discovered. According to the two potential miRNAs, we found the 240 and 457 predicted mRNAs targeted by potential hsa-miR-22-3p and hsa-miR-130b-3p, respectively (Supplementary file 7B and C). By matching the predicted mRNAs with DEmRNAs from the experiments, 58 mRNAs were identified to be regulated by hsa-miR-22-3p and hsa-miR-130b-3p. On the basis of the above data, the lncRNA-miRNA-mRNA ceRNA network was established and is shown in Fig. 7A.

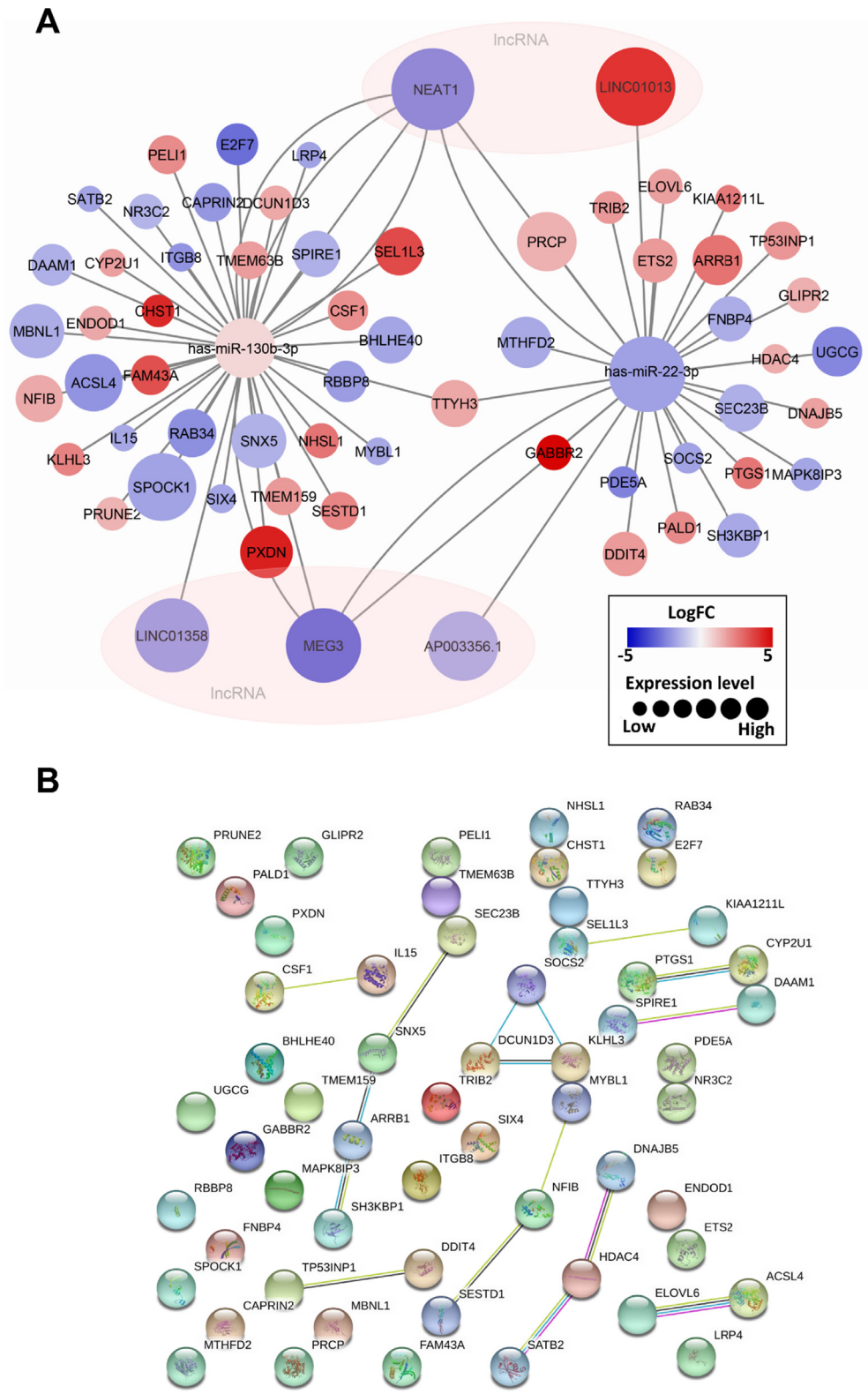

Fig. 7. (A) The lncRNA-miRNA-mRNA ceRNA network. There are 5 potential lncRNAs (NEAT1, LINC01013, LINC01358, MEG3, and AP003356.1), 2 potential miRNAs (hsa-miR-22-3p and hsa-miR-130b-3p), and 58 potential mRNAs identified in this ceRNA network. (B) The protein–protein interaction (PPI) network based on the mRNAs in ceRNA network. The top 10 hub genes based on the PPI network were ELOVL6, ACSL4, ARRB1, SH3KBP1, PTGS1, CYP2U1, SNX5, DCUN1D3, KLHL3, and SOCS2.

Moreover, we mapped these potential targeted genes based on the STRING database for establishment of PPI network according to the miRNAs in the established ceRNA network aiming to better understanding their relationship (Fig. 7B). The top 10 hub genes were ELOVL6, ACSL4, ARRB1, SH3KBP1, PTGS1, CYP2U1, SNX5, DCUN1D3, KLHL3, and SOCS2.

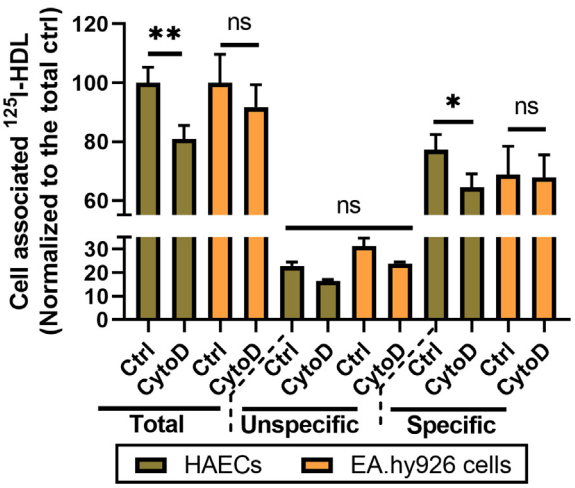

Fig. 8. Cytochalasin D significantly decreased both total and specific HDL cellular association in HAECs, but not in EA.hy926 cells. HAECs and EA.hy926 cells were seeded at a density of 0.1×10^6 cells/well in 24-well plates for 48 h. Cells were then treated with cytochalasin D (Sigma, C8273) or control (0.1% DMSO) for 24 h. Cells were then incubated with 10 μg/mL of ^{125}I-HDL for 1 h in the absence (total) or presence (unspecific) of 40-fold excess of unlabeled HDL. Specific HDL cellular association was calculated by subtracting unspecific values from total values. Data are shown as mean ± SD from three independent experiments, each performed in triplicate in case of the HDL cellular association assay (C). *P < 0.05, **P < 0.01, and ns not significant (ANOVA with Bonferroni test).

3.7. Cytochalasin D significantly inhibits HDL cellular association in HAECs but not EA.hy926 cells

According to the results above, we found that genes related to cell − cell adhesion, ECM organization, extracellular structure organization and homophilic cell adhesion are highly expressed in HAECs compared to EA.hy926 cells. Furthermore, significantly enriched pathways Ras signaling pathway and Rap1 signaling pathway in HAECs contributed to endocytosis, cell adhesion, migration and so on. HDL binding and uptake by ECs are involved in various processes, such as adhesion and endocytosis (Wang et al., 2020). Therefore, we hypothesized that HAECs would exhibit stronger HDL cellular endocytosis than EA.hy926 cells. We treated ECs with a endocytosis inhibitor cytochalasin D (a potent inhibitor of actin polymerization) to verify whether HAECs have stronger response to HDL cellular association than EA.hy926 cells. As shown in Fig. 8, cytochalasin D significantly decreased both total and specific HDL cellular association in HAECs, but not in EA.hy926 cells.

4. Discussion

RNA-seq data provide advantages in both biological status and genome coverage for the comprehensive understanding of the transcriptome. In this study, we used RNA-seq technology to identify DEGs between HAECs and EA.hy926 cells, suggesting immortal EA.hy926 cells have significant difference in gene expression profile compared to primary HAECs, which is consistent with other reports (Chi et al., 2003; Lidington et al., 1999).

In GO enrichment analysis, we found that DEGs highly expressed in HAECs are involved in much more GO terms compared to EA.hy926 cells. These GO terms are related to the properties of endothelial cells, such as cell adhesion, extracellular matrix (ECM)/structure organization, endothelial cell proliferation/development/migration, vascular development, and so on. However, the DEGs highly expressed in EA.hy926 cells are involved in RTK activity, integrin binding, and reproductive development. Along the same line, both KEGG pathways analysis and GSEA enrichment analysis also showed that enriched pathway Ras signaling pathway and Rap1 signaling pathway in HAECs contributed to endocytosis, cell–cell junction, cell migration, while enriched pathway MAPK signaling pathway in EA.hy926 cells contributed to the cell cycle and proliferation. These data suggest that EA.hy926 cells are lacking of some endothelial characters compared to primary endothelial cells.

In both KEGG pathways analysis and GSEA enrichment analysis, we found that DEGs highly expressed in HAECs are distributed in 2 pathways, namely the Rap1 signaling pathway and Ras signaling pathway. Ras signaling pathway is involved in vascular malformations and hemorrhagic stroke, p38MAPK activation and heat-shock protein 27 (HSP27) phosphorylation (Chang et al., 2006; Li et al., 2018; Sawada et al., 2015). It was reported that the small G-protein Rap1 played a critical role in endothelial function, such as NO release, NO-dependent vasodilation, and endothelial barrier function which is regulated by cell–cell adhesions and their connection to the actin cytoskeleton (Lakshmikanthan et al., 2015; Pannekoek et al., 2014). Therefore, the two pathways are very important for endothelial function, although they are also lowly expressed in EA.hy926 cells.

We also established the ceRNA network, and further set up PPI network according to 58 potential mRNAs in ceRNA network. Among them, 2 potential miRNAs (hsa-miR-22-3p and hsa-miR-130b-3p) and 5 lncRNAs (NEAT1, LINC01013, LINC01358, MEG3, and AP003356.1) are very interesting. The miR-22 protected endothelial cells from injury by targeting NLRP3 (NOD-, LRR- and pyrin domain-containing protein 3) in a rat model of coronary heart disease (Huang et al., 2017). The miR-130 activated angiogenesis by targeting c-MYB in vascular endothelial cells (Yang et al., 2018). To the best of our knowledge, there are limited studies on the role of the two miRNAs in endothelial functions. It would be valuable to investigate the effects of miR-22 and miR-130 on endocytosis, cell–cell junction and other endothelial functions. It was reported that lncRNA NEAT1 inhibited oxidative stress-induced vascular endothelial cell injury (Zhang et al., 2019), facilitated survival and angiogenesis in oxygen-glucose deprivation (OGD)-induced brain microvascular endothelial cells (Zhou et al., 2019). MEG3 attenuated the angiotensin II-induced injury of HUVEC (Song et al., 2019), protected endothelial function by regulating the DNA damage response (Shihabudeen Haider Ali et al., 2019), prevented vascular endothelial cell senescence (Boon et al., 2016; Lan et al., 2019) and so on. It remains to further investigate the molecular mechanism of the effect of lnc-RNA-miRNA-mRNA on endothelial functions, for which our ceRNA network might provide a genomic basis.

As shown in enrichment analysis, we found that genes related to cell − cell adhesion, endocytosis, and Rap1 signaling pathway are highly expressed in HAECs compared to EA.hy926 cells. Furthermore, Rap1 plays a critical role in actin cytoskeleton (Lakshmikanthan et al., 2015; Pannekoek et al., 2014). These data suggest that HAECs may have a stronger response to endothelial binding and endocytosis compared to EA.hy926 cells. Interestingly, our data showed that an endocytosis inhibitor, cytochalasin D, by suppressing actin polymerization indeed significantly decreased endocytosis of HDL in HAECs, but not EA.hy926 cells.

5. Conclusions

This study identified DEGs between HAECs and EA.hy926 cells, and found enrichment of the Ras signaling pathway and Rap1 signaling pathway in HAECs, established ceRNA network and suggested that HAECs may have a stronger response to endothelial binding and endocytosis compared to EA.hy926 cells. This study will provide a genomic

basis for investigators to choose suitable EC models to reach their research goals.

Funding

This work was supported by the Cultivation project for clinical medicine of the integrated traditional Chinese and western medicine and Cultivation project for education team of internal medicine of the integrated traditional Chinese and western medicine in the first-term subjects with special support in the first-class universities in Guizhou province (Qin Jiao Gao Fa No. 2017-158).

CRediT authorship contribution statement

Dongdong Wang: Conceptualization, Methodology. **Zhu Chen:** . **Andy Wai Kan Yeung:** . **Atanas G. Atanasov:** Conceptualization, Methodology.

Declaration of Competing Interest

Given their roles as Current Research in Biotechnology Editor-in-Chief and Executive Editor, Atanas G. Atanasov and Dongdong Wang, respectively, had no involvement in the peer review process of this article and have had no access to information regarding its peer review process.

Edtorial disclosure

Given their roles as Current Research in Biotechnology Editor-in-Chief and Executive Editor, Atanas G. Atanasov and Dongdong Wang, respectively, had no involvement in the peer review process of this article and have had no access to information regarding its peer review process.

Appendix A. Supplementary material

Supplementary data to this article can be found online at https://doi.org/10.1016/j.crbiot.2021.05.001.

References

Ahn, K., Pan, S., Beningo, K., Hupe, D., 1995. A permanent human cell line (EA.hy926) preserves the characteristics of endothelin converting enzyme from primary human umbilical vein endothelial cells. Life Sci. 56 (26), 2331–2341.

Ala, U., Karreth, F.A., Bosia, C., Pagnani, A., Taulli, R., Leopold, V., Tay, Y., Provero, P., Zecchina, R., Pandolfi, P.P., 2013. Integrated transcriptional and competitive endogenous RNA networks are cross-regulated in permissive molecular environments. Proc. Natl. Acad. Sci. U. S. A. 110 (18), 7154–7159.

Boon, R.A., Hofmann, P., Michalik, K.M., Lozano-Vidal, N., Berghauser, D., Fischer, A., Knau, A., Jae, N., Schurmann, C., Dimmeler, S., 2016. Long noncoding RNA Meg3 controls endothelial cell aging and function: implications for regenerative angiogenesis. J. Am. Coll. Cardiol. 68 (23), 2589–2591.

Bouis, D., Hospers, G.A., Meijer, C., Molema, G., Mulder, N.H., 2001. Endothelium in vitro: a review of human vascular endothelial cell lines for blood vessel-related research. Angiogenesis 4 (2), 91–102.

Campochiaro, P.A., 2013. Ocular neovascularization. J. Mol. Med. (Berl.) 91 (3), 311–321.

Chang, X., Firestone, G.L., Bjeldanes, L.F., 2006. Inhibition of growth factor-induced Ras signaling in vascular endothelial cells and angiogenesis by 3,3'-diindolylmethane. Carcinogenesis 27 (3), 541–550.

Chi, J.T., Chang, H.Y., Haraldsen, G., Jahnsen, F.L., Troyanskaya, O.G., Chang, D.S., Wang, Z., Rockson, S.G., van de Rijn, M., Botstein, D., Brown, P.O., 2003. Endothelial cell diversity revealed by global expression profiling. Proc. Natl. Acad. Sci. U. S. A. 100 (19), 10623–10628.

Chrissobolis, S., Miller, A.A., Drummond, G.R., Kemp-Harper, B.K., Sobey, C.G., 2011. Oxidative stress and endothelial dysfunction in cerebrovascular disease. Front Biosci. (Landmark Ed) 16, 1733–1745.

Falkenberg, K.D., Rohlenova, K., Luo, Y., Carmeliet, P., 2019. The metabolic engine of endothelial cells. Nat. Metabolism 1 (10), 937–946.

Gustincich, S., Sandelin, A., Plessy, C., Katayama, S., Simone, R., Lazarevic, D., Hayashizaki, Y., Carninci, P., 2006. The complexity of the mammalian transcriptome. J. Physiol. 575 (Pt 2), 321–332.

Huang, W.Q., Wei, P., Lin, R.Q., Huang, F., 2017. Protective effects of microrna-22 against endothelial cell injury by targeting NLRP3 through suppression of the inflammasome signaling pathway in a rat model of coronary heart disease. Cell. Physiol. Biochem. 43 (4), 1346–1358.

Ji, X., Li, P., Fuscoe, J.C., Chen, G., Xiao, W., Shi, L., Ning, B., Liu, Z., Hong, H., Wu, J., Liu, J., Guo, L., Kreil, D.P., Labaj, P.P., Zhong, L., Bao, W., Huang, Y., He, J., Zhao, Y., Tong, W., Shi, T., 2020. A comprehensive rat transcriptome built from large scale RNA-seq-based annotation. Nucleic Acids Res..

Kaissarian, N., Kang, J., Shu, L., Ferraz, M.J., Aerts, J.M., Shayman, J.A., 2018. Dissociation of globotriaosylceramide and impaired endothelial function in alpha-galactosidase-A deficient EA.hy926 cells. Mol. Genet. Metab. 125 (4), 338–344.

Klemke, R.L., Yebra, M., Bayna, E.M., Cheresh, D.A., 1994. Receptor tyrosine kinase signaling required for integrin alpha v beta 5-directed cell motility but not adhesion on vitronectin. J. Cell Biol. 127 (3), 859–866.

Kraehling, J.R., Chidlow, J.H., Rajagopal, C., Sugiyama, M.G., Fowler, J.W., Lee, M.Y., Zhang, X., Ramirez, C.M., Park, E.J., Tao, B., Chen, K., Kuruvilla, L., Larrivee, B., Folta-Stogniew, E., Ola, R., Rotllan, N., Zhou, W., Nagle, M.W., Herz, J., Williams, K. J., Eichmann, A., Lee, W.L., Fernandez-Hernando, C., Sessa, W.C., 2016. Genome-wide RNAi screen reveals ALK1 mediates LDL uptake and transcytosis in endothelial cells. Nat. Commun. 7, 13516.

Lakshmikanthan, S., Zheng, X., Nishijima, Y., Sobczak, M., Szabo, A., Vasquez-Vivar, J., Zhang, D.X., Chrzanowska-Wodnicka, M., 2015. Rap1 promotes endothelial mechanosensing complex formation, NO release and normal endothelial function. EMBO Rep. 16 (5), 628–637.

Lan, Y., Li, Y.J., Li, D.J., Li, P., Wang, J.Y., Diao, Y.P., Ye, G.D., Li, Y.F., 2019. Long noncoding RNA MEG3 prevents vascular endothelial cell senescence by impairing miR-128-dependent Girdin downregulation. Am. J. Physiol. Cell Physiol. 316 (6), C830–C843.

Law, C.W., Chen, Y., Shi, W., Smyth, G.K., 2014. voom: Precision weights unlock linear model analysis tools for RNA-seq read counts. Genome Biol. 15 (2), R29.

Li, Q.F., Decker-Rockefeller, B., Bajaj, A., Pumiglia, K., 2018. Activation of Ras in the vascular endothelium induces brain vascular malformations and hemorrhagic stroke. Cell Rep 24 (11), 2869–2882.

Lidington, E.A., Moyes, D.L., McCormack, A.M., Rose, M.L., 1999. A comparison of primary endothelial cells and endothelial cell lines for studies of immune interactions. Transpl. Immunol. 7 (4), 239–246.

Malyszko, J., 2010. Mechanism of endothelial dysfunction in chronic kidney disease. Clin. Chim. Acta 411 (19–20), 1412–1420.

Mortazavi, A., Williams, B.A., McCue, K., Schaeffer, L., Wold, B., 2008. Mapping and quantifying mammalian transcriptomes by RNA-Seq. Nat. Methods 5 (7), 621–628.

Pan, Q., Shai, O., Lee, L.J., Frey, B.J., Blencowe, B.J., 2008. Deep surveying of alternative splicing complexity in the human transcriptome by high-throughput sequencing. Nat. Genet. 40 (12), 1413–1415.

Pannekoek, W.J., Post, A., Bos, J.L., 2014. Rap1 signaling in endothelial barrier control. Cell Adh Migr 8 (2), 100–107.

Potente, M., Gerhardt, H., Carmeliet, P., 2011. Basic and therapeutic aspects of angiogenesis. Cell 146 (6), 873–887.

Sawada, J., Li, F., Komatsu, M., 2015. R-Ras inhibits VEGF-induced p38MAPK activation and HSP27 phosphorylation in endothelial cells. J. Vasc. Res. 52 (5), 347–359.

Shao, Y., Saredy, J., Yang, W.Y., Sun, Y., Lu, Y., Saaoud, F., Drummer, C.t., Johnson, C., Xu, K., Jiang, X., Wang, H., Yang, X., 2020. Vascular Endothelial Cells and Innate Immunity. Arterioscler Thromb Vasc Biol 40(6), e138-e152.

Shihabudeen Haider Ali, M.S., Cheng, X., Moran, M., Haemmig, S., Naldrett, M.J., Alvarez, S., Feinberg, M.W., Sun, X., 2019. LncRNA Meg3 protects endothelial function by regulating the DNA damage response. Nucleic Acids Res 47(3), 1505-1522.

Song, J., Huang, S., Wang, K., Li, W., Pao, L., Chen, F., Zhao, X., 2019. Long non-coding RNA MEG3 attenuates the angiotensin ii-induced injury of human umbilical vein endothelial cells by interacting with p53. Front. Genet. 10, 78.

Subramanian, A., Tamayo, P., Mootha, V.K., Mukherjee, S., Ebert, B.L., Gillette, M.A., Paulovich, A., Pomeroy, S.L., Golub, T.R., Lander, E.S., Mesirov, J.P., 2005. Gene set enrichment analysis: a knowledge-based approach for interpreting genome-wide expression profiles. Proc. Natl. Acad. Sci. U. S. A. 102 (43), 15545–15550.

Szklarczyk, D., Morris, J.H., Cook, H., Kuhn, M., Wyder, S., Simonovic, M., Santos, A., Doncheva, N.T., Roth, A., Bork, P., Jensen, L.J., von Mering, C., 2017. The STRING database in 2017: quality-controlled protein-protein association networks, made broadly accessible. Nucleic Acids Res. 45 (D1), D362–D368.

Tabit, C.E., Chung, W.B., Hamburg, N.M., Vita, J.A., 2010. Endothelial dysfunction in diabetes mellitus: molecular mechanisms and clinical implications. Rev. Endocr. Metab. Disord. 11 (1), 61–74.

Thornhill, M.H., Li, J., Haskard, D.O., 1993. Leucocyte endothelial cell adhesion: a study comparing human umbilical vein endothelial cells and the endothelial cell line EA-hy-926. Scand. J. Immunol. 38 (3), 279–286.

Uhrin, P., Wang, D., Mocan, A., Waltenberger, B., Breuss, J.M., Tewari, D., Mihaly-Bison, J., Huminiecki, Ł., Starzyński, R.R., Tzvetkov, N.T., Horbańczuk, J., Atanasov, A.G., 2018. Vascular smooth muscle cell proliferation as a therapeutic target. Part 2: Natural products inhibiting proliferation. Biotechnol. Adv. 36 (6), 1608–1621.

Van Dreden, P., Epsilonlalamy, I., Gerotziafas, G.T., 2017. The role of tissue factor in cancer-related hypercoagulability, tumor growth, angiogenesis and metastasis and future therapeutic strategies. Crit. Rev. Oncog. 22 (3–4), 219–248.

Voelkel, N.F., Gomez-Arroyo, J., 2014. The role of vascular endothelial growth factor in pulmonary arterial hypertension. The angiogenesis paradox. Am. J. Respir. Cell Mol. Biol. 51 (4), 474–484.

Wang, D., Rohrer, L., von Eckardstein, A., 2020. Sphingosine-1-phosphate receptors 1 and 3 regulate the expression of scavenger receptor B1 in human aortic endothelial cells. bioRxiv, 2020.2004.2023.058263. doi: https://doi.org/10.1101/2020.04.23.058263

Wang, D., Uhrin, P., Mocan, A., Waltenberger, B., Breuss, J.M., Tewari, D., Mihaly-Bison, J., Huminiecki, Ł., Starzyński, R.R., Tzvetkov, N.T., Horbańczuk, J., Atanasov, A.G., 2018. Vascular smooth muscle cell proliferation as a therapeutic target. Part 1: molecular targets and pathways. Biotechnol. Adv. 36 (6), 1586–1607.

Yang, H., Zhang, H., Ge, S., Ning, T., Bai, M., Li, J., Li, S., Sun, W., Deng, T., Zhang, L., Ying, G., Ba, Y., 2018. Exosome-derived miR-130a activates angiogenesis in gastric cancer by targeting C-MYB in vascular endothelial cells. Mol. Ther. 26 (10), 2466–2475.

Yu, F., Fu, R., Liu, L., Wang, X., Wu, T., Shen, W., Gui, Z., Mo, X., Fang, B., Xia, L., 2019. Leptin-induced angiogenesis of EA.Hy926 endothelial cells via the Akt and Wnt signaling pathways in vitro and in vivo. Front. Pharmacol. 10, 1275.

Zhang, M., Wang, X., Yao, J., Qiu, Z., 2019. Long non-coding RNA NEAT1 inhibits oxidative stress-induced vascular endothelial cell injury by activating the miR-181d-5p/CDKN3 axis. Artif. Cells Nanomed. Biotechnol. 47 (1), 3129–3137.

Zhou, Z.W., Zheng, L.J., Ren, X., Li, A.P., Zhou, W.S., 2019. LncRNA NEAT1 facilitates survival and angiogenesis in oxygen-glucose deprivation (OGD)-induced brain microvascular endothelial cells (BMECs) via targeting miR-377 and upregulating SIRT1, VEGFA, and BCL-XL. Brain Res. 1707, 90–98.